Atmos. Chem. Phys., 16, 11787–11805, 2016
www.atmos-chem-phys.net/16/11787/2016/
doi:10.5194/acp-16-11787-2016

Atmospheric Chemistry and Physics Open Access EGU

Trends analysis of PM source contributions and chemical tracers in NE Spain during 2004–2014: a multi-exponential approach

Marco Pandolfi[1], Andrés Alastuey[1], Noemi Pérez[1], Cristina Reche[1], Iria Castro[1], Victor Shatalov[2], and Xavier Querol[1]

[1]Institute of Environmental Assessment and Water Research, c/Jordi-Girona 18-26, 08034 Barcelona, Spain
[2]Meteorological Synthesizing Centre, East, 2nd Roshchinsky proezd, 8/5, 115419 Moscow, Russia

Correspondence to: Marco Pandolfi (marco.pandolfi@idaea.csic.es)

Received: 14 January 2016 – Published in Atmos. Chem. Phys. Discuss.: 29 March 2016
Revised: 1 September 2016 – Accepted: 8 September 2016 – Published: 22 September 2016

Abstract. In this work for the first time data from two twin stations (Barcelona, urban background, and Montseny, regional background), located in the northeast (NE) of Spain, were used to study the trends of the concentrations of different chemical species in PM_{10} and $PM_{2.5}$ along with the trends of the PM_{10} source contributions from the positive matrix factorization (PMF) model. Eleven years of chemical data (2004–2014) were used for this study. Trends of both species concentrations and source contributions were studied using the Mann–Kendall test for linear trends and a new approach based on multi-exponential fit of the data. Despite the fact that different PM fractions ($PM_{2.5}$, PM_{10}) showed linear decreasing trends at both stations, the contributions of specific sources of pollutants and of their chemical tracers showed exponential decreasing trends. The different types of trends observed reflected the different effectiveness and/or time of implementation of the measures taken to reduce the concentrations of atmospheric pollutants. Moreover, the trends of the contributions of specific sources such as those related with industrial activities and with primary energy consumption mirrored the effect of the financial crisis in Spain from 2008. The sources that showed statistically significant downward trends at both Barcelona (BCN) and Montseny (MSY) during 2004–2014 were secondary sulfate, secondary nitrate, and V–Ni-bearing source. The contributions from these sources decreased exponentially during the considered period, indicating that the observed reductions were not gradual and consistent over time. Conversely, the trends were less steep at the end of the period compared to the beginning, thus likely indicating the attainment of a lower limit. Moreover, statistically significant decreasing trends were observed for the contributions to PM from the industrial/traffic source at MSY (mixed metallurgy and road traffic) and from the industrial (metallurgy mainly) source at BCN. These sources were clearly linked with anthropogenic activities, and the observed decreasing trends confirmed the effectiveness of pollution control measures implemented at European or regional/local levels. Conversely, at regional level, the contributions from sources mostly linked with natural processes, such as aged marine and aged organics, did not show statistically significant trends. The trends observed for the PM_{10} source contributions reflected the trends observed for the chemical tracers of these pollutant sources well.

1 Introduction

Meeting air quality (AQ) standards is one of the major environmental objectives to protect people from breathing air with high levels of pollution. Many studies have been published in these last years showing clearly that the concentrations of particulate matter (PM), and other air pollutants such as sulfur dioxide (SO_2) and carbon monoxide (CO), have markedly decreased during the last 15 years in many European countries (EEA, 2013; Barmpadimos et al., 2012; Cusack et al., 2012; Querol et al., 2014; Guerreiro et al., 2014 among others). Cusack et al. (2012) reported the reduction in $PM_{2.5}$ concentrations observed at regional background (RB) stations in Spain and across Europe, and, in most cases, the observed reduction was gradual and consistent over time, implying the success of cleaner anthropogenic activities. Barm-

padimos et al. (2012) have also shown that PM_{10} concentrations decreased at a number of urban background (UB) and rural background stations in five European countries. Henschel et al. (2013) reported the dramatic decrease in SO_2 levels in six European cities, which reflected the reduction in sulfur content in fuels, as part of European legislation, coupled with the shift towards the use of cleaner fuels. EEA (2013) also reported general decreases in NO_2 concentrations, even if they were lower compared to PM. However, Henschel et al. (2015) showed that the NO_x concentrations at traffic sites in many European cities remained unchanged, underlining the need of further regulative measures to meet the air quality standards for this pollutant. In fact an important proportion of the European population lives in areas exceeding the AQ standards for the annual limit value of NO_2, the daily limit value of PM_{10}, and the health protection objective of O_3 (EEA, 2013, 2015). PM_{10} and NO_2 are still exceeded mostly in urban areas, and especially at traffic sites (Harrison et al., 2008; Williams and Carslaw, 2011; EEA, 2013; among others). In Spain, for example, it has been reported that more than 90 % of the NO_2 exceedances can be attributed to road traffic emissions (Querol et al., 2012). Guerreiro et al. (2014) furthermore evidenced the notable reduction of ambient air concentration of SO_2, CO, and Pb using data available in Airbase (EEA, 2013), covering 38 European countries. Querol et al. (2014) reported trends for 73 measurement sites across Spain including regional background (RB), urban background (UB), traffic stations (TS), and industrial sites (IND). They observed marked downward trends for the concentrations of PM_{10}, $PM_{2.5}$, CO, and SO_2 at most of the RB, UB, TR, and IND sites considered. Similarly, Salvador et al. (2012) detected statistically significant downward trends for the concentrations of SO_2, NO_x, CO and $PM_{2.5}$ at most of the urban and urban-background monitoring sites in the Madrid metropolitan area during 1999–2008. Cusack et al. (2012) and Querol et al. (2014) have also shown the statistically significant decreasing trends for many trace elements (Pb, Cu, Zn, Mn, Cd, As, Sn, V, Ni, Cr) at regional level in the northeast (NE) of Spain since 2002.

The observed reduction of air pollutants across Europe is the result of efficient emission abatement strategies, as for example those implemented in the Industrial Emission Directive (IPPC – Integrated Pollution Prevention and Control – and subsequent Industrial Emission Directive 1996/61/EC and 2008/1/EC), the Large Combustion Plant Directive (LCPD; 2001/80/EC), the EURO standards on road traffic emission (1998/69/EC, 2002/80/EC, 2007/715/EC), and the IMO (International Maritime Organization) directive on sulfur content in fuel and SO_x and NO_x emissions from ships (IMO, 2011; Directive 2005/33/EC). Additionally, the financial crisis, causing mainly a reduction of the primary energy consumption from 2008 to 2009, contributed to the decrease of the ambient concentration of pollutants observed in Spain (Querol et al., 2014).

Moreover, national and regional measures for AQ have been taken in many European countries. In Spain a national AQ plan was approved in 2011 and updated in 2013 by the Council of Ministers of the government of Spain. Furthermore, 45 regional and 3 local (city-scale) AQ plans have been implemented since 2004 in Spain. These AQ plans have mostly focused on improving AQ at major city centers and specific industrial areas.

Thanks to the aforementioned measures there is clear evidence that the concentrations of PM in many European countries have markedly decreased during the last decades. However, in spite of the above policy efforts, a significant proportion of the urban population in Europe lives in areas exceeding the World Health Organization (WHO) AQ standards, for example for $PM_{2.5}$, PM_{10}, and O_3 (EEA, 2013, 2015).

The analysis of the trends of the concentration of air pollutants helps in evaluating the effectiveness of specific AQ measures depending on the pollutant considered. Examining data over time also makes it possible to predict future frequencies and/or rates of occurrence making future projections. For the abovementioned reasons, the feasibility of studying the trends of the contributions to PM mass from specific pollutant sources, along with the trends of the chemical tracers of these sources, is especially attractive.

To the best of our knowledge, in the majority of studies dealing with trend analysis, linear fits were applied by using Mann–Kendall (MK) or Theil–Sen methods (Theil, 1950; Sen, 1968), the latter being available, for example, in the Openair software (Carslaw, 2012; Carslaw and Ropkins, 2012). However, a linear fit of data does not always properly represent the observed trends. As we will show, different abatement strategies and periods of implementation may change from one pollutant to another, thus leading to different trends for different pollutants, even over the same period. Thus, a nonlinear fit of the data may be strongly recommended at times.

The main aim of this work was to study the trends of PM_{10} source contributions and of specific chemical species in both PM_{10} and $PM_{2.5}$ using both the consensus methodology (Mann–Kendall) and the nonlinear approach. The data of Spanish national emissions and energy consumption were also evaluated to interpret the observed trends. Understanding past trends may be relevant for devising new strategies for air pollution abatement. PM chemical speciated data collected from 2004 to 2014 at regional (Montseny, NE Spain) and urban (Barcelona, NE Spain) sites were used with this aim. The positive matrix factorization (PMF) model was used to apportion ambient PM_{10} concentrations into pollutant sources. The PMF model, as other receptor models, is widely used as a powerful tool to help policymakers to design more targeted approaches to protecting public health. Thus, the novelty of this study lies mainly (a) in the opportunity to study the trends of pollutant source contributions from the PMF model at two twin stations representative of the urban and regional environments in the western Mediter-

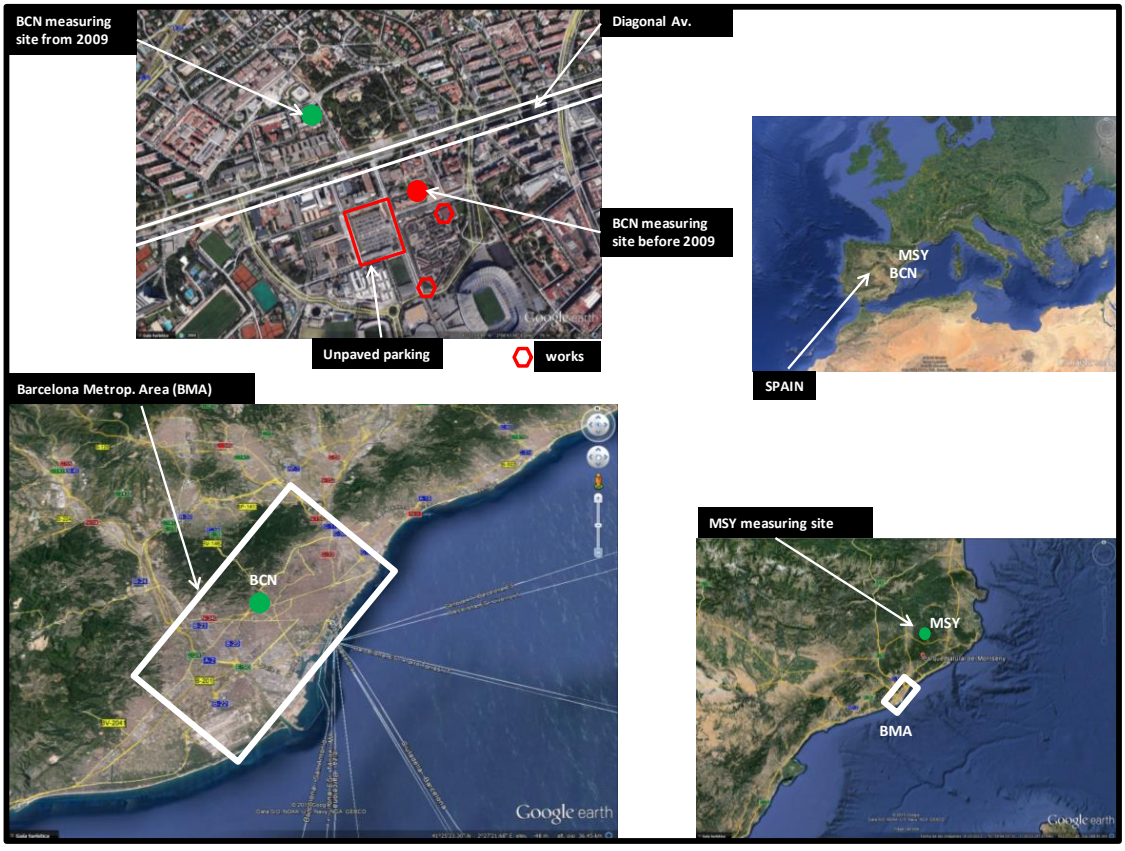

Figure 1. Location of the Barcelona (BCN) and Montseny (MSY) measuring stations. Red full circle highlights the location of the BCN measuring station before 2009. Green full circle highlights the new location of the BCN (from 2009) and MSY measuring stations.

ranean, and, (b) in the use of a novel nonlinear approach for trend studies.

2 Measurement sites and methodology

2.1 Measurement sites

The Montseny measurement station (MSY, 41°46′45.63″ N, 02°21′28.92″ E; 720 m a.s.l.) is a regional background site in the NE of Spain, located in a regional natural park about 50 km to the NNE of the city of Barcelona (BCN) and 25 km from the Mediterranean coast (Fig. 1). This site is representative of the typical regional background conditions of the western Mediterranean Basin (WMB), characterized by severe pollution episodes affecting not only the coastal sites closest to the emission sources, but also the more elevated rural and remote areas inland (i.e., Pérez et al., 2008; Pey et al., 2010; Pandolfi et al., 2011, 2014). This station is part of the ACTRIS (www.actris.net) and GAW (www.wmo.int/gaw) networks, of the EMEP Program (http://www.emep.int/) and of the measuring network of the government of Catalonia.

The Barcelona measurement station (BCN, 41°23′24.01″ N, 02°06′58.06″ E; 68 m a.s.l.) is an urban background measurement site influenced by vehicular emissions from one of the main avenues of the city (Diagonal Avenue) located at a distance of around 300 m (cf. Fig. 1). The BCN measurement site is part of the air quality measuring network of the government of Catalonia. The metropolitan area of Barcelona (BMA), with nearly 4.5 million inhabitants, covers a strip 8 km wide between the Mediterranean Sea and the coastal mountain range. Several industrial zones, power plants, and highways are located in the area, making this region one of the most polluted in the WMB (i.e., Querol et al., 2008; Amato et al., 2009; Pandolfi et al., 2012, 2013, 2014). At BCN the location of the measuring station changed in 2009 when it was moved by around 500 m (cf. Fig. 1). The effect of this change on PM measurements performed at BCN will be discussed later.

2.2 Real-time and gravimetric PM measurements

Real-time PM concentrations were continuously measured at 1h resolution by optical particle counters (OPCs) using GRIMM spectrometers (GRIMM 180 at MSY, and GRIMM 1107, 1129, and 180 at BCN). Hourly PM concentrations

were corrected by comparison with 24 h gravimetric mass measurements of PM_x (Alastuey et al., 2011).

For gravimetric measurements, 24 h PMx samples were collected at both stations every 3–4 days on 150 mm quartz micro-fiber filters (Pallflex QAT and Whatman) with high-volume samplers (DIGITEL DH80 and/or MCV CAV-A/MSb at 30 $m^3 h^{-1}$). The mass of PM_{10} and $PM_{2.5}$ samples collected on filters was determined using the EN 12341 and the EN14907 gravimetric procedures, respectively.

2.2.1 PM chemical speciated data

Once the gravimetric mass was determined from filters, the samples were analyzed with different techniques, including acidic digestion (1/2 of each filter; $HNO_3 : HF : HClO_4$), water extraction of soluble anions (1/2 of each filter), and thermal-optical analysis (1.5 cm^2 sections). Inductively coupled atomic emission spectrometry, ICP-AES, (IRIS Advantage TJA Solutions, THERMO) was used for the determination of the major elements (Al, Ca, Fe, K, Na, Mg, S, Ti, P), and inductively coupled plasma mass spectrometry, ICP-MS, (X Series II, THERMO) for the trace elements (Li, Ti, V, Cr, Mn, Co, Ni, Cu, Zn, As, Se, Rb, Sr, Cd, Sn, Sb, Ba, rare earths, Pb, Bi, Th, U). Ionic chromatography was used for the concentrations of NO_3^-, SO_4^{2-}, and Cl^-, whereas NH_4^+ was determined using a specific electrode MODEL 710 A+, THERMO Orion. The levels of organic carbon (OC) and elemental carbon (EC) were determined using a thermal-optical carbon analyzer (SUNSET), using protocol EUSAAR_2 (Cavalli et al., 2010). Other analytical details may be found in Querol et al. (2008).

Following the above procedures, a total of 1093 PM_{10} and 794 $PM_{2.5}$ filters were collected and analyzed at MSY during the period 2004–2014. At BCN the collected filters were 1037 and 1063 in PM_{10} and $PM_{2.5}$, respectively.

2.3 Positive matrix factorization (PMF) model

The PMF model (PMFv5.0, EPA) was applied to the collected daily PM_{10} speciated data for source identification and apportionment at both sites. Detailed information about the PMF model can be found in literature (Paatero and Tapper, 1994; Paatero, 1997; Paatero and Hopke, 2003; Paatero et al., 2005). The PMF model is a factor analytical tool, reducing the dimension of the input matrix to a limited number of factors (or sources), and it is based on the weighted least-squares method. Thus, most important in PMF applications is the estimation of uncertainties of the chemical species included in the input matrix. In the present study, individual uncertainties and detection limits were calculated as in Escrig et al. (2009) and Amato et al. (2009). Thus, both the analytical uncertainties and the standard deviations of species concentrations in the blank filters were considered in the uncertainties calculations. The signal-to-noise ratio (S/N) was estimated starting from the calculated uncertainties and used as a criterion ($S/N > 2$) for selecting the species used within the PMF model. In order to avoid any bias in the PMF results, the data matrix was uncensored (Paatero, 2004). The PMF was run in robust mode (Paatero, 1997), and rotational ambiguity was handled by means of the F_{PEAK} parameter (Paatero et al., 2005). The optimal number of sources was selected by inspecting the variation of the objective function Q (defined as the ratio between residuals and errors in each data value) with a varying number of sources (i.e., Paatero et al., 2002) and by studying the physical meaningfulness of the calculated factors.

2.4 Mann–Kendall (MK) fit

The purpose of the Mann–Kendall (MK) test (Mann, 1945; Kendall, 1975; Gilbert, 1987) is to statistically assess whether there is a monotonic upward or downward trend of the variable of interest with time. A monotonic upward (downward) trend means that the variable consistently increases (decreases) through time. The Mann–Kendall test tests the null hypothesis H_0 of no trend, i.e., the observations are randomly ordered in time, against the alternative hypothesis, H_1, where there is an increasing or decreasing monotonic trend. The main advantage of the Mann–Kendall test is that data need not conform to any particular distribution and missing data are allowed. To estimate the slope of the trend, Sen's method was used (Salmi et al., 2002).

2.5 Multi-exponential (ME) fit

A program aiming at studying trends by means of multi-exponential fit of the data was developed within the Task Force on Measurements and Modelling (TFMM) by the Meteorological Synthesizing Centre – East (MSC-E; http://www.msceast.org/) group (Shatalov et al., 2015). The TFMM together with the Task Force on Emission Inventories and Projections (TFEIP), the Task Force on Integrated Assessment Modelling (TFIAM), and Task Force on Hemispheric Transport of Air Pollution (TFHTAP) provide fora for discussion and scientific exchange in support of the EMEP (European Monitoring and Evaluation Programme; http://www.emep.int/) work plan, which is a scientifically based and policy-driven program under the Convention on Long-range Transboundary Air Pollution (CLRTAP; http://www.unece.org/env/lrtap/lrtap_h1.html) to promote international co-operation and to solve transboundary air pollution problems. The TFMM was established in 2000 to evaluate measurements and modeling and to further develop working methods and tools. In this context, five EMEP centers are undertaking efforts in support of the EMEP work plan, namely the MSC-E, the Centre on Emission Inventories and Projections (CEIP; http://www.ceip.at/), the Chemical Coordinating Centre (CCC; http://www.nilu.no/projects/ccc/), the Meteorological Synthesizing Centre – West (MSC-W; http://emep.int/mscw/index_mscw.html), and the Centre for In-

tegrated Assessment Modelling (CIAM; http://www.iiasa.ac.at/~rains/ciam.html). In 2014 the TFMM initiated an exercise dedicated to assessing the efficiency of CLRTAP air pollution mitigation strategies over the past 20 years, evaluating the benefit of its main policy instruments. Within this exercise a piece of software was made available by EMEP/MSC-E, with the aim of studying nonlinear trends. Annual, monthly, and daily resolution data can be analyzed with the help of this program. Since in this paper we will apply the program to annual averages of species concentrations and source contributions, we restrict the description of the multi-exponential approximations to this case. In particular, seasonal variations are not taken into consideration. The basic equations solved by the program for this particular case (annual averages) are reported below:

$$C_t = a_1 \cdot \exp\left(-\frac{t}{\tau_1}\right) + a_2 \cdot \exp\left(-\frac{t}{\tau_2}\right) + \ldots + a_n \cdot \exp\left(-\frac{t}{\tau_n}\right) + \omega_t, \quad (1)$$

where C_t are the values of the considered time series, with $t = 1, \ldots, \mathrm{N}$, N being the length of the series (years), τ_n are the characteristic times of the considered exponential, a_n are constants, and ω_t are the residue values. In the case of single exponential decay ($n = 1$) the characteristic time τ is the time at which the pollutant concentration is reduced to 1/e (i.e., 0.3678) times its initial value. The main difference between linear and exponential fit is that in the latter case, the trend is not gradual and constant over time. For an exponential trend the absolute ($\mu g\,m^{-3}$) reduction per year decreases with time, being the highest at the beginning of the period. Conversely, for a linear fit, the absolute reduction is constant over time. For an exponential fit, the lower the characteristic time τ, the more rapidly the considered quantity vanishes. Deviations from single exponential fit can be taken into account introducing more exponential terms. In this work, for example, two exponential terms were sometimes used. In this case two characteristic times are calculated by the software. If the decrease of the considered quantity is very sharp at the beginning of the period (more than single exponential), then both τ_1 and τ_2 are positive. Conversely, one exponential term with negative τ takes possible increase of the quantity at the end of the period into account. Both τ_n and a_n are calculated by the program by means of the least-squares method, minimizing the residue ω, and the statistically significance of the exponential fit is provided by means of the p value. The number of exponential terms that should be included into the approximation can be evaluated using F-statistics (i.e., Smith, 2002). For example, the F-statistics for the evaluation of the statistical significance of the second term in equation (1) for $n = 2$ can be calculated as

$$F = \frac{(\mathrm{SS}_1 - \mathrm{SS}_2)}{2 \cdot s}, \quad (2)$$

where SS_1 and SS_2 are sums of squares of residual component for approximations with one and two exponential terms, respectively, and s is the estimate of standard deviation of residual component. This statistic approximately follows the Fisher distribution, with 2 and N -2° of freedom. The second exponential is considered to be significant if F exceeds the corresponding threshold value at the chosen significance level.

The following parameters can be calculated from Eq. (1):

$$\text{total reduction: TR} = \frac{(C_{\mathrm{beg}} - C_{\mathrm{end}})}{C_{\mathrm{beg}}} = 1 - \frac{C_{\mathrm{end}}}{C_{\mathrm{beg}}} \quad (3)$$

$$\text{annual reduction for year } i: \; R_i = \frac{\Delta C_i}{C_i} = 1 - \frac{C_{i+1}}{C_i} \quad (4)$$

$$\text{average annual reduction: } R_{\mathrm{av}} = 1 - \left(\frac{C_{\mathrm{end}}}{C_{\mathrm{beg}}}\right)^{\frac{1}{N-1}}, \quad (5)$$

where C_{beg} and C_{end} are the first and the last points, respectively, of the exponential fit. The formula for the calculation of the average annual reduction takes into account that the ratio $C_i + 1/C_i$ is a multiplicative quantity, so that geometrical mean of ratios should be used. The relative contribution of residues (residual component: RC) is calculated as the standard deviation of the ratios between the residue values of the fit ω_t (cf. Eq. 1) and the main component of the fit.

The MSC-E also proposed a statistic that measures the deviation of the obtained trend from the linear one (nonlinearity parameter: NL). A trend is defined as linear if the NL parameter is lower than 10 %, indicating a small difference between ME and MK fits (Shatalov et al., 2015). In the following, the reported trends were analyzed using the MK test for NL < 10 % and the ME test for NL > 10 %. A more detailed description of the multi-exponential approach is available in the TFMM wiki and in the MSC-E technical report 2015 (Shatalov et al., 2015).

3 Results

Results are presented and discussed in the following order. In Sect. 3.1, we compare the trends at both stations of PM_x concentrations from optical particle counters (OPCs; annual data coverage around 90 %) and from 24 h gravimetric samples (filters; annual data coverage around 20–30 %). This comparison will demonstrate the feasibility of studying trends of chemical species concentrations from filters despite the relatively low annual data coverage. In Sect. 3.2, we compare the magnitude of the trend of $PM_{2.5}$ concentrations at MSY during 2004–2014 (period selected for this study) with the magnitude of trends calculated at the same station over different periods, namely 2002–2010 (the period used in Cusack et al., 2012) and 2002–2014 (representing the largest period of gravimetric $PM_{2.5}$ measurements available at MSY station at the time of writing). This comparison was performed in order to study the differences in the trends over short periods (9

Table 1. Trends of different PM mass fractions from gravimetry (grav) and optical (OPC) measurements at BCN (italic) and MSY (2004-2014). TR (%) is the total reduction; RC (%) is the residual component. Significance of the trends following the Mann–Kendall test: *** (p value < 0.001), ** (p value < 0.01), * (p value < 0.05), + (p value < 0.1).

PM_x	PM_x		Mann–Kendall fit			
Fraction	Conc. 2004 ($\mu g m^{-3}$)	Conc. 2014 ($\mu g m^{-3}$)	p value	Trend ($\mu g m^{-3} yr^{-1}$)	TR (%)	RC (%)
PM_{10} (grav.)	*41.1*	*19.2*	***	*−2.83*	*59.2*	*8.5*
	19.2	13.9		−0.17	10.5	17.6
$PM_{2.5}$ (grav.)	*31.6*	*13.2*	***	*−2.03*	*60.1*	*7.9*
	16.2	9.8	+	−0.33	25.6	17.3
PM_{10} (OPC)	*39.1*	*19.8*	***	*−2.20*	*50.4*	*10.0*
	18.6	12.3		−0.13	7.8	16.9
$PM_{2.5}$ (OPC)	*27.1*	*12.9*	**	*−1.55*	*49.6*	*9.8*
	16.5	9.3	+	−0.26	21.2	17.5

to 13 years). The gravimetric concentrations of $PM_{2.5}$ measured at MSY were used with this aim. Then, in Sect. 3.3, we present and discuss the trends at both stations of chemical species from filters in both PM_{10} and $PM_{2.5}$. In Sect. 4.0 we discuss the sources of pollutants identified by the PMF model in PM_{10} at both sites. Finally, we present and discuss the trends of PM_{10} source contributions at BCN and MSY (Sect. 4.1), providing possible explanations for the observed trends. Conclusions are reported in Sect. 5.

3.1 Trends of PM: comparison between gravimetric and real-time optical measurements

Annual data coverage is an important factor to take into account in order to study trends of a given parameter. The gravimetric PM measurements, from which chemical speciated data are obtained, are typically performed with rather low frequency over 1 year. In our case, the annual data coverage of gravimetric measurements was around 20–30 % at both Barcelona and Montseny. In this section, we compare the trends of PM concentrations from gravimetric and real-time optical measurements (Table 1). Given that the trends of the considered PM_x fractions were linear at both sites (NL < 10 %), only results from MK test were reported in Table 1. However, we will show later (Sect. 4.1) that the contributions from specific PM_{10} pollutant sources, mainly those related with anthropogenic activities, showed nonlinear (i.e., exponential) decreasing trends, thus mirroring the different effectiveness of the mitigation strategies depending on the source of pollutants considered.

As reported in Table 1, statistically significant decreasing trends were observed for the considered PM size fractions at BCN ($-2.20\,\mu g\,m^{-3}\,yr^{-1}$ with $p < 0.001$ for PM_{10} and $-1.55\,\mu g\,m^{-3}\,yr^{-1}$ with $p < 0.01$ for $PM_{2.5}$ from OPC measurements), whereas at Montseny, only the $PM_{2.5}$ fraction showed a slightly significant decreasing trend ($-0.26\,\mu g\,m^{-3}\,yr^{-1}$; $p < 0.1$ from OPC measurements). Total reduction (TR) ranged between 50.4 % (OPC PM_{10} at BCN) and 7.8 % (OPC PM_{10} at MSY), and the residual component (RC) was lower than 18 %, reflecting the goodness of the linear (MK) fit used. It must be noted that the higher p-values, magnitude of the trends, and TR observed at BCN compared to MSY was likely due to the change of the measuring station in 2009 in BCN (cf. Fig. 1). Based on the comparison between simultaneous PM_x chemical speciated data collected at both BCN measurement sites during 1 month (not shown), we concluded that after 2009, the BCN measuring site was less affected by mineral matter and, to a lesser extent, by road traffic emissions, both being important sources of PM in Barcelona. In Fig. 1 we highlight the proximity of the BCN measuring station before 2009 to an unpaved parking area and different construction works. The effect of the change of the station in BCN in 2009 on PM_{10} gravimetric measurements is reported in the Supplement (Fig. S1). However, despite the change of the station, the comparison between BCN and MSY for specific chemical species and pollutant sources not linked with mineral matter and road traffic emissions was possible.

Table 1 shows that the p-values calculated using gravimetric and OPC measurements were the same despite the different annual data coverage. The differences in the magnitude of the trends were 22 and 24 % between gravimetric and OPC PM_{10} and $PM_{2.5}$ measurements, respectively, at BCN and 24 and 21 %, respectively, at MSY. Relative differences of total reduction (TR) ranged between 24 % for gravimetric and OPC PM_{10} measurements at MSY and 15 % for PM_{10} at BCN. Thus, despite the different data coverage, the magnitude of the trends and TR calculated from OPCs and gravimetric measurements were rather similar. Other PM mass fractions (PM_{1-10} and $PM_{2.5-10}$) and PM ratios (PM_1 / PM_{10} and $PM_{2.5}$ / PM_{10}) at MSY showed nonstatistically significant trends.

Table 2. Mann–Kendall and multi-exponential trends of different chemical species in PM_{10} at BCN (italic) and MSY. Type of trend: linear (L), single exponential (SE), double exponential (DE); a ($\mu g m^{-3}$) and τ (yr) are the constants and the characteristic times, respectively, of the exponential data fittings; NL (%) is the nonlinearity; TR (%) is the total reduction; RC (%) is the residual component; ns denotes not statistically significant; ni denotes not included. Significance of the trends: *** (p value < 0.001), ** (p value < 0.01), * (p value < 0.05), + (p value < 0.1).

PM_{10} (BCN; MSY)			Mann–Kendall fit				Multi-exponential fit				
Specie	Concentration 2004 ($\mu g m^{-3}$)	Concentration 2014 ($\mu g m^{-3}$)	Fit type	NL (%)	p value	Trend ($\mu g m^{-3} yr^{-1}$)	a ($\mu g m^{-3}$)	τ (yr)	Trend ($\mu g m^{-3} yr^{-1}$)	TR (%)	RC (%)
Pb	*0.02685*	*0.00694*	SE	*27*	***		*0.03246*	*6.12*	*−0.00222*	*80*	*17*
	0.00481	0.00190	SE	11	**		0.00553	10.22	−0.00031	62	13
Cd	*0.00043*	*0.00015*	SE	*19*	***		*0.00048*	*7.59*	*−3.10E-5*	*73*	*17*
	0.00017	0.00006	SE	18	**		0.00018	7.92	−1.12E-5	72	16
As	*0.00094*	*0.00036*	SE	*14*	***		*0.00118*	*9.11*	*−7.07E-5*	*67*	*11*
	0.00029	0.00017	L	< 10	***	−1.29E-5				50	9
V	*0.01116*	*0.00454*	SE	*12*	**		*0.01502*	*10.04*	*−0.00086*	*63*	*17*
	0.00328	0.00175	L	< 10	**	−0.00022				59	15
Ni	*0.00531*	*0.00284*	SE	*11*	***		*0.00678*	*10.61*	*−0.00037*	*61*	*16*
	0.00155	0.00100	L	< 10	**	−7.10E-5				43	20
Sn	ni	ni									
	0.00127	0.00057	L	< 10	*	−3.65E-5				39	16
Cu	ni	ni									
	0.00420	0.00216	L	< 10	*	−0.00014				36	20
Sb	ni	ni									
	0.00058	0.00025	SE	11	**		0.00064	10.46	−3.57E-5	62	13
SO_4^{2-}	*5.74436*	*2.28596*	SE	*12*	***		*6.56033*	*9.81*	*−0.37868*	*64*	*12*
	2.84849	1.67712	L	< 10	**	−0.11836				42	18
NO_3^-	*5.07816*	*1.72401*	SE	*12*	**		*6.49890*	*9.83*	*−0.37484*	*64*	*15*
	1.80724	0.67419	L	< 10	**	−0.10593				54	13
NH_4^+	*1.92062*	*0.57008*	SE	*12*	***		*1.90645*	*9.64*	*−0.11095*	*65*	*14*
	1.14268	0.40135	SE	13	*		1.28868	9.26	−0.07640	66	22
Al_2O_3	ni	ni									
	0.72357	0.46382	L	< 10	*	−0.02383				34	18
Ca	ni	ni									
	0.42703	0.28279	L	< 10	*	−0.01638				38	17
Fe	ni	ni									
	0.22371	0.14895	L	< 10	+	−0.00593				6	44
Na	*1.02188*	*0.77408*	L	*< 10*	*	*−0.03943*				*34*	*12*
					ns						

3.2 Trends of PM: comparison among different periods

In this study we used the period 2004–2014 for trends analysis, given that gravimetric $PM_{2.5}$ measurements at BCN have been available since 2004. Conversely, at MSY $PM_{2.5}$, gravimetric measurements started in 2002. Figure 2 shows the trends of $PM_{2.5}$ concentrations at MSY, calculated using the MK test for the three different periods. The ME test was not used here given that the observed trends were linear (NL < 10 %). The period 2002–2010 was the period considered in the paper from Cusack et al. (2012) presenting the trends of $PM_{2.5}$ gravimetric mass and chemical species at MSY. The period 2002–2014 is the largest period, with $PM_{2.5}$ filter measurements available at the time of writing. The trend observed at MSY for the $PM_{2.5}$ fraction during 2004–2014 confirmed what was already observed by Cusack et al. (2012) at the same station for the period 2002–2010. In Cusack et al. (2012), the MK test provided a decreasing trend of around $-0.66\,\mu g\,m^{-3}\,yr^{-1}$ at 0.01 significance level (TR of 35 %). During the periods 2004–2014 and 2002–2014, decreasing trends of $-0.33\,\mu g\,m^{-3}\,yr^{-1}$ ($p < 0.1$; TR of 26 %) and $-0.37\,\mu g\,m^{-3}\,yr^{-1}$ ($p < 0.05$; TR of 31 %), respectively, were observed. Thus, a statistically significant trend for $PM_{2.5}$ mass at regional level can be observed, even when considering different periods, thus confirming the effectiveness of mitigation measures together with the effect of the economic crisis in Spain from 2008. However, it should be noted that the statistical significance of the trends observed for the larger periods was lower compared to Cusack et al. (2012). The difference observed in the magnitude of the trends during 2004–2014 compared to the results provided by Cusack et al. (2012) was mainly due to the increase of $PM_{2.5}$

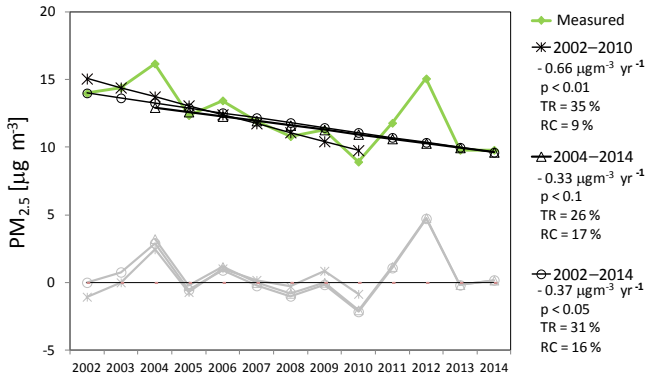

Figure 2. Mann–Kendall fit of $PM_{2.5}$ trends at MSY station for the periods 2002–2010 (as in Cusack et al., 2012), 2004–2014 (this work), and 2002–2014 (largest period available in the time of writing). The magnitude of the trends ($\mu g m^{-3} yr^{-1}$), p value, total reduction (TR), and residual component (RC) are reported. Significance of the trends following the Mann–Kendall test: *** (p value < 0.001), ** (p value < 0.01), * (p value < 0.05), + (p value < 0.1).

mass concentration in 2012 (cf. Fig. 2). Chemical $PM_{2.5}$ speciated data revealed that this increase was partly driven by organic matter showing a mean annual concentration in 2012 higher by around 20 % compared to the 2004–2014 average.

3.3 Trends of chemical species

The trends of the annual mean concentrations of chemical species at BCN and MSY are reported in Table 2 (for PM_{10}) and Table 3 (for $PM_{2.5}$). Figure 3 (for BCN) and Fig. 4 (for MSY) show the trends of chemical species in PM_{10}. In Tables 2 and 3 and Figs. 3 and 4, only the species that have statistically significant trends were reported.

As already noted we assume that the change of the station in BCN in 2009 affected the trends of the concentrations of OC, EC, Cu, Sn, Sb, and Zn (mainly traffic tracers), Al_2O_3, Ca, Mg, Ti, Rb, Sr (crustal elements related with both natural and anthropogenic sources), and Fe (traffic and crustal tracer). These chemical species at BCN were removed from Tables 2 and 3 and from Fig. 3.

Other species measured in BCN were not affected by the change of the station. These are SO_4^{2-}, NH_4^+, V, Ni (related with heavy oil combustion in the study area according to source apportionment results, cf. Par. 4), Pb, Cd, and As (related with industrial/metallurgy activities), Na and Cl (sea spray), and NO_3^-. Although nitrate particles in Barcelona were mainly from traffic, the concentrations of these particles were not strongly affected by the change of the station due to their secondary origin. The MSY station will be considered as reference station given that no location change occurred at this monitoring site during the study period.

Statistically significant exponential trends ($p < 0.01$ or 0.001) were mainly observed for the industrial tracers (Pb, Cd, As) in both PM_{10} and $PM_{2.5}$. For these elements TR was high and around 50–80 % in PM_{10} and 67–81 % in $PM_{2.5}$. The RCs were lower than 20 %, thus suggesting the goodness of the exponential fits used to study the trends of these species. Exponential fits were needed on average, indicating that the trends were not gradual and consistent over time and that the effectiveness of the control measures for these pollutants was stronger at the beginning of the period under study (2004–2009 approximately) compared to the end of the period (Figs. 3 and 4). This is also evident by comparing the linear MK fit (dashed black line) with the ME fit (red line) in Figs. 3 and 4. In PM_{10} the magnitudes of the trends ranged from -0.00222 (Pb; $p < 0.001$) to -3.10×10^{-5} $\mu g m^{-3} yr^{-1}$ (Cd; $p < 0.001$) at BCN and from -0.00031 (Pb; $p < 0.01$) to -1.12×10^{-5} $\mu g m^{-3} yr^{-1}$ (Cd; $p < 0.01$) at MSY. In $PM_{2.5}$ the magnitudes of the trends were similar and ranged between -0.00163 $\mu g m^{-3} yr^{-1}$ (Pb; $p < 0.001$) and -3.11×10^{-5} $\mu g m^{-3} yr^{-1}$ (Cd; $p < 0.001$) at BCN and between -0.00049 $\mu g m^{-3} yr^{-1}$ (Pb; $p < 0.001$) and -1.35×10^{-5} $\mu g m^{-3} yr^{-1}$ (Cd; $p < 0.001$) at MSY. Similar magnitude of the trends for these species in both PM fractions at both sites confirmed the common origin of these elements and the impact at regional scale of industrial sources. For Pb and Cd, the characteristic time (τ) of the exponential trends was similar at both sites, whereas for As it was higher due to the slightly less intense exponential downward trend observed for As compared to Cd and Pb. Note that the PMF analysis (cf. Sect. 4) revealed that the concentrations of As were explained by multiple sources (especially at BCN), whereas the industrial/metallurgy source alone explained more than around 70 % of Pb and Cd concentrations (not shown). The implementation of the IPPC Directive in 2008 in Spain is the most probable cause for this downward trend. The decrease observed for Pb, Cd, and As may also be attributed to a decrease in the emissions from industrial production (smelters; Querol et al., 2007) at a regional scale around Barcelona.

The concentrations of V and Ni in Barcelona in both PM_{10} and $PM_{2.5}$ fractions showed very similar exponential decreasing trends. Similar characteristic times (around 10–11 years), TR (around 59–63 %), and RC (15–17 %) in both fractions suggested the common and mainly fine origin of these two elements. At MSY, V and Ni showed linear trends likely because of the higher distance of the MSY station to the sources of V and Ni (shipping and, before 2008, energy production) compared to BCN. Note also that the NL parameter for BCN V and Ni was around 10–12 %, indicating that in this case the exponential fit did not differ very much from the linear one. Total reduction for V and Ni at MSY was around 59–64 and 42–43 %, respectively, and RCs were lower than 24 %.

Sn and Cu in PM_{10} at MSY showed very similar behavior by decreasing linearly with time, with TR around 36–39 % and RC around 16–20 %. Decreasing rates of -3.65×10^{-5} ($p < 0.05$) and -0.00014 $\mu g m^{-3} yr^{-1}$ ($p < 0.05$) were ob-

Table 3. Mann–Kendall and multi-exponential trends of different chemical species in $PM_{2.5}$ at BCN (italic) and MSY. Type of trend: linear (L), single exponential (SE), double exponential (DE); a ($\mu g m^{-3}$) and τ (yr) are the constants and the characteristic times, respectively, of the exponential data fittings; NL (%) is the nonlinearity; TR (%) is the total reduction; RC (%) is the residual component; ns denotes not statistically significant; ni denotes not included. Significance of the trends: *** (p value < 0.001), ** (p value < 0.01), * (p value < 0.05), + (p value < 0.1).

$PM_{2.5}$ (*BCN*;MSY)			Mann–Kendall fit				Multi-exponential fit				
Specie	Concentration 2004 ($\mu g m^{-3}$)	Concentration 2014 ($\mu g m^{-3}$)	Fit type	NL (%)	p value	Trend ($\mu g m^{-3} yr^{-1}$)	a ($\mu g m^{-3}$)	τ (yr)	Trend ($\mu g m^{-3} yr^{-1}$)	TR (%)	RC (%)
Pb	*0.02117*	*0.00500*	SE	*27*	***		*0.02390*	*6.24*	*−0.00163*	*80*	*13*
	0.00642	0.00149	SE	28	***		0.00716	6.08	−0.00049	81	18
Cd	*0.00041*	*0.00011*	SE	*23*	***		*0.00047*	*6.81*	*−3.11E-5*	*77*	*13*
	0.00020	0.00005	SE	23	***		0.00020	6.77	−1.35E-5	77	18
As	*0.00069*	*0.00027*	SE	*14*	***		*0.00091*	*9.00*	*−5.43E-5*	*67*	*11*
	0.00029	0.00013	SE	15	**		0.00033	8.56	−2.04E-5	69	19
V	*0.00823*	*0.00368*	SE	*11*	**		*0.01121*	*11.13*	*−0.00061*	*59*	*16*
	0.00271	0.00130	L	< 10	**	−0.00017				64	24
Ni	*0.00402*	*0.00185*	SE	*10*	**		*0.00498*	*11.23*	*−0.00027*	*59*	*15*
	0.00189	0.00080	SE	13	**		0.00205	9.36	−0.00012	42	21
Sn	ni	ni									
	0.00157	0.00043	L	< 10	***	−0.00084				61	12
Cu	ni	ni									
	0.00394	0.00113	SE	14	**		0.00426	8.99	−0.00026	67	13
Sb	ni	ni									
	0.00053	0.00015	DE	48	**		0.00069	4.52	−3.86E-5	70	16
							1.3E-6	−2.50			
SO_4^{2-}	*4.86564*	*1.92388*	SE	*12*	***		*5.64582*	*9.69*	*−0.32778*	*64*	*9*
	2.98922	1.43381	L	< 10	**	−0.16222				54	15
NO_3^-	*3.45513*	*0.86002*	SE	*19*	***		*4.14459*	*7.61*	*−0.26753*	*73*	*16*
	1.66095	0.29452	SE	30	***		1.96014	5.81	−0.13550	82	21
NH_4^+	*2.19735*	*0.68393*	SE	*11*	***		*2.27813*	*10.53*	*−0.12701*	*61*	*15*
	1.39366	0.48049	SE	18	**		1.62588	7.94	−0.10266	72	14
Al_2O_3	ni	ni									
	0.30245	0.10153	SE	13	*		0.26678	9.36	−0.01574	66	35
Ca	ni	ni									
	0.11478	0.06540	L	< 10	+	−0.00494				50	33
Fe	ni	ni									
	0.09679	0.03716	L	< 10	*	−0.00504				61	31
Na	*0.27476*	*0.17863*	L	< 10	+	*−0.01247*				*41*	*15*
	0.13091	0.07252	L	< 10	*	−0.00584				45	18

served in PM_{10} for Sn and Cu, respectively. In $PM_{2.5}$, the concentrations of Sn and Cu decreased markedly compared to PM_{10} at the rate of -0.00084 ($p < 0.001$) and $-0.00026\,\mu g\,m^{-3}\,yr^{-1}$ ($p < 0.01$), respectively. This difference could be explained by possible sources of coarser Sn and Cu, which reduced the magnitude of the trends in PM_{10} mass fraction. Sb showed marked decreasing trends in both PM mass fractions compared to Sn and Cu, with TR around 62–70 %. The magnitude of the trend for Sb was similar in both fractions and around $-3.57 \div -3.86 \times 10^{-5}\,\mu g\,m^{-3}\,yr^{-1}$. The concentrations of Sb were better fitted with exponential curves (SE with $p < 0.01$ in PM_{10} and DE with $p < 0.01$ in $PM_{2.5}$). The DE fit for Sb in $PM_{2.5}$ had one positive and one negative characteristic time; the latter was needed to explain the slight increase in Sb concentrations at the end of the considered period. The marked decreasing trend observed for Sb compared to other traffic tracers could be explained by a progressive reduction of Sb contained in the vehicle brakes. Cr did not show a statistically significant trend in both PM fractions.

Sulfate (SO_4^{2-}) and ammonium (NH_4^+) particles' concentrations showed very similar behavior in $PM_{2.5}$ and PM_{10} size fractions due to their fine nature. In BCN, the magnitudes of the trends were -0.37868 ($p < 0.001$) and $-0.11095\,\mu g\,m^{-3}\,yr^{-1}$ ($p < 0.001$) for SO_4^{2-} and NH_4^+, respectively, in PM_{10} and -0.32778 ($p < 0.001$) and $-0.12701\,\mu g\,m^{-3}\,yr^{-1}$ ($p < 0.001$), respectively, in $PM_{2.5}$. The trends were SE with very similar characteristic times (9.64–9.81 years in PM_{10} and 9.69–10.53 years in $PM_{2.5}$), TR (64–65 % in PM_{10} and 61–64 % in $PM_{2.5}$), and RC (12–14 % in PM_{10} and 9–15 % in $PM_{2.5}$). At MSY, the magnitudes of the trends of SO_4^{2-} and NH_4^+ and their statistical

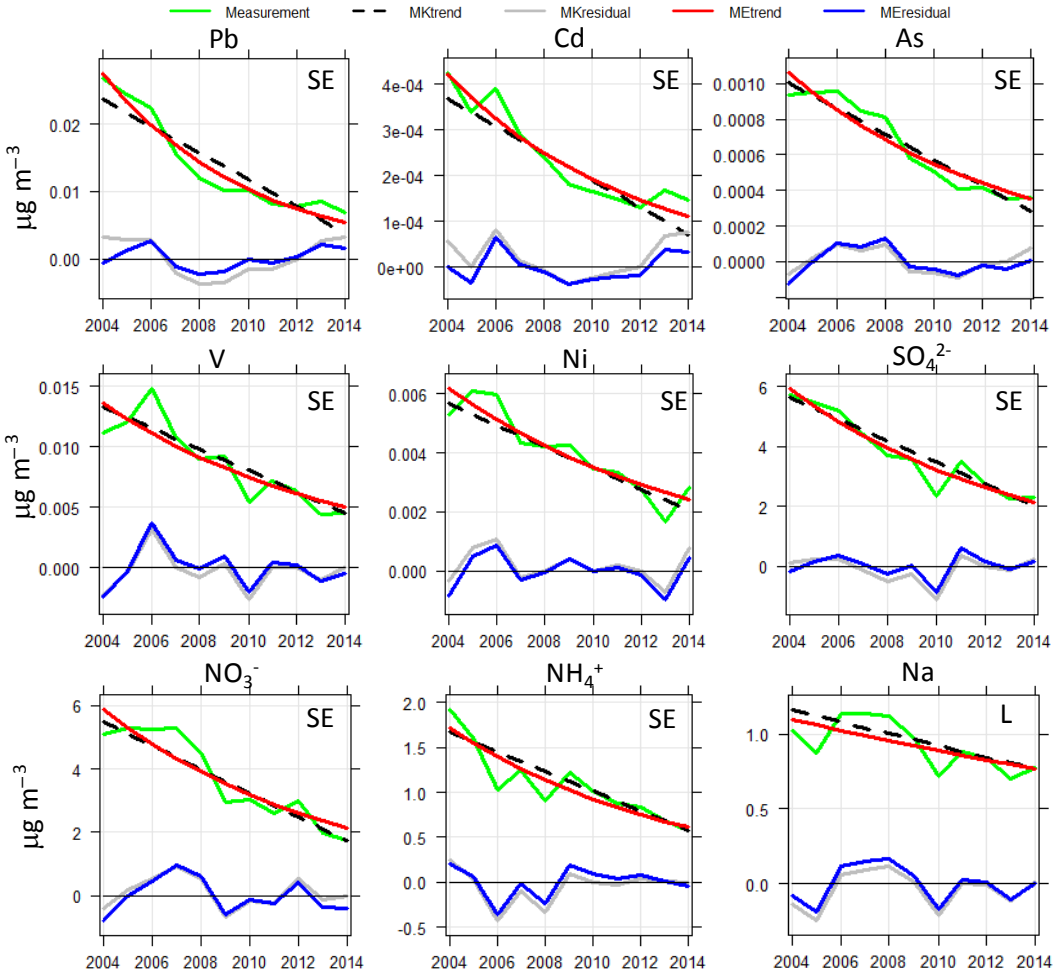

Figure 3. Mann–Kendall (MK) and multi-exponential (ME) trends for chemical species at BCN in PM_{10}. Measured concentration (green line); multi-exponential trend (red line); multi-exponential residuals (blue line); Mann–Kendall trend (black line); Mann–Kendall residuals (gray line). Trend type: linear (L), single exponential (SE), double exponential (DE).

significance were lower compared to BCN in both fractions. Moreover, at MSY, the trends were linear for SO_4^{2-} in both fractions (as for V and Ni). These differences could be explained by the distance of MSY to direct specific sources of sulfate, such as shipping, compared to BCN, thus slightly reducing the magnitude and the statistical significance of the trend of SO_4^{2-} at regional level. It is also interesting to note the similitude between the characteristic times of the exponential fits for V and Ni and SO_4^{2-} in both PM fractions at BCN, suggesting the main common origin of these chemical species. Possible reasons for the observed reduction in the concentrations of ambient sulfate in and around Barcelona will be discussed later.

Fine NO_3^- (Table 3) showed statistically significant SE trends similar at both sites with $p < 0.001$, TR around 73–82 %, RC around 16–21 %, and characteristic times around 5.8–7.6 years. In PM_{10} the TRs were lower and around 54–64 % and the fits were linear at MSY and SE at BCN. The SE fit in PM_{10} at BCN provided a characteristic time around 9.8 years, which was higher compared to the τ obtained for the fine mode (7.6 years), thus indicating that fine NO_3^- had a more pronounced downward trend compared to PM_{10} NO_3^-.

For the mineral species (Al_2O_3, Ca, Fe) linear (with the exception of Al_2O_3 in $PM_{2.5}$ which was SE) and statistically significant decreasing trends were detected at MSY. On average the TR was higher in the fine fraction, ranging from 50 for Ca to 66 % for Al_2O_3, compared to PM_{10} (6–38 % cf. Table 2). A downward decreasing trend for crustal material in $PM_{2.5}$ at MSY was also reported by Cusack et al. (2012) for the period 2002–2010 and by Querol et al. (2014) for the period 2001–2012. These trends were probably driven by weather conditions associated with negative North Atlantic Oscillation (NAO) index (iNAO) that could be the cause for this slight reduction observed in crustal material. Pey et al. (2013) found a correlation between iNAO (calculated between June and September) and the contribution of Saharan

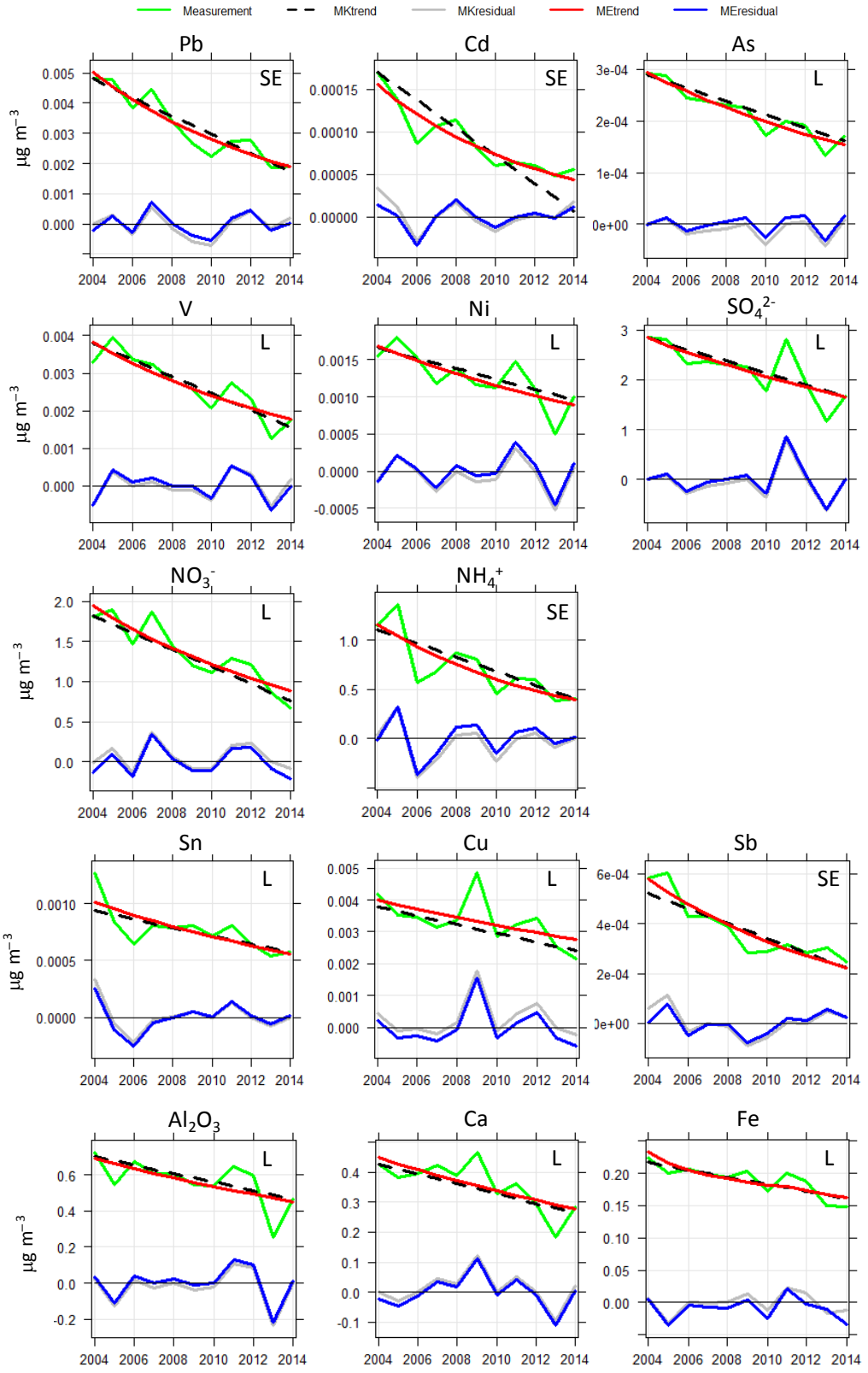

Figure 4. Mann–Kendall (MK) and multi-exponential (ME) trends for chemical species at MSY in PM_{10}. Measured concentration (green line); multi-exponential trend (red line); multi-exponential residuals (blue line); Mann–Kendall trend (black line); Mann–Kendall residuals (gray line). Trend type: linear (L), single exponential (SE), double exponential (DE).

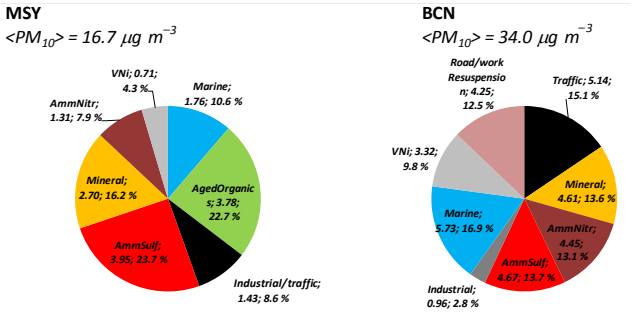

Figure 5. Source contributions from PMF model in PM_{10} at Montseny (MSY) and Barcelona (BCN). Mean values during 2004–2014. Values reported are sources in $\mu g\,m^{-3}$ and %.

dust to PM_{10} mass in the NE of Spain, and showed that the more negative the iNAO is, the lower the dust contribution to PM. The iNAO was unusually negative during the period 2008–2012 (http://www.cpc.ncep.noaa.gov/products/precip/CWlink/pna/norm.nao.monthly.b5001.current.ascii), thus likely contributing to the explanation of the observed trends of crustal elements. Moreover, negative NAO can favor the presence of fronts that can sweep the Iberian Peninsula from west to east, causing stronger winds and less stagnant conditions, thus favoring the dispersion of pollutants. In addition, as suggested by Cusack et al. (2012), it could also be hypothesized that some part of the crustal material measured at MSY is a product of the construction industry. The construction industry in Spain has been especially affected by the current economic recession, and crustal material produced by this industry may have contributed to the crustal load in $PM_{2.5}$. For example the number of home construction works in Barcelona during 2008–2014 (from the beginning of the economic crisis; mean number of works of 1281) reduced by around 75 % compared to the period 2000–2007 (mean number of works of 5187; http://www.bcn.cat/estadistica/castella/dades/timm/construccio/index.htm). The fact that the total reduction calculated for mineral elements reported in Tables 2 and 3 was higher in $PM_{2.5}$ compared to PM_{10} could corroborate the hypothesis of an anthropogenic contribution to the mineral matter measured at MSY.

Finally, Na concentrations showed linear decreasing trends at both sites, with the exception of PM_{10} Na at MSY. Other species at MSY such as OC and EC did not show statistically significant trends. Consider that the concentrations of EC at MSY are very low and around an annual mean of 0.2–0.3 $\mu g\,m^{-3}$. Both anthropogenic activity and biomass burning were expected to contribute to this chemical species. Concerning OC, the lack of trend was probably due to the contribution from biogenic sources to the concentration of this species at regional level.

4 PMF source profiles and contributions

Eight and seven sources were detected at BCN and MSY, respectively, in PM_{10} from PMF model. The absolute and relative contributions of these sources to the measured PM_{10} mass were reported in Fig. 5, whereas the chemical profiles of the detected sources were reported in the Supplement (Fig. S2).

Some sources were common at both BCN and MSY. These are secondary sulfate (secondary inorganic source traced by SO_4^{2-} and NH_4^+ and contributing 3.95 (23.7 %) and 4.67 $\mu g\,m^{-3}$ (13.7 %) at MSY and BCN, respectively), secondary nitrate (secondary inorganic source traced by NO_3^- and NH_4^+ and contributing 1.31(7.9 %) and 4.45 $\mu g\,m^{-3}$ (13.1 %) at MSY and BCN, respectively), V–Ni-bearing source (traced mainly by V, Ni, and SO_4^{2-}, it represents the direct emissions from heavy oil combustion and contributed 0.71 (4.3 %) and 3.32 $\mu g\,m^{-3}$ (9.8 %) at MSY and BCN, respectively), mineral (traced by typical crustal elements such as Al, Ca, Ti, Rb, and Sr and contributing 2.70 (16.2 %) and 4.61 $\mu g\,m^{-3}$ (13.6 %) at MSY and BCN, respectively), and aged marine (traced by Na and Cl mainly with contributions from SO_4^{2-} and NO_3^- and contributing 1.76 (10.6 %) and 5.73 $\mu g\,m^{-3}$ (16.9 %) at MSY and BCN, respectively). Sources detected at MSY but not at BCN were the industrial/traffic source (traced by EC, OC, Cr, Cu, Zn, As, Cd, Sn, Sb, and Pb), which included contributions from anthropogenic sources such as road traffic and metallurgic industries and contributed 1.43 $\mu g\,m^{-3}$ (8.6 %), and aged organics (traced mainly by OC and EC), with maxima in summer indicating mainly a biogenic origin and contributing 3.78 $\mu g\,m^{-3}$ (22.7 %). The ratio OC : EC in the industrial/traffic and aged organic source profiles at MSY were 4.2 and 11.7, respectively, thus indicating a strong influence of aged particles in the latter source, with the former source being more fresh. The statistic of the OC : EC ratio based on chemical data at MSY is reported in the Supplement (Fig. S3). Mean and median values of OC : EC ratio at MSY were 9.1 and 7.8, respectively.

Finally, some sources were detected at BCN but not at MSY: traffic (traced mainly by C_{nm}, Cr, Cu, Sb and Fe) contributing 5.14 $\mu g\,m^{-3}$ (15.1 %), road/work resuspension (traced by both crustal elements, mainly Ca, and traffic tracers such as Sb, Cu, and Sn) contributing 4.25 $\mu g\,m^{-3}$ (12.5 %), and industrial/metallurgy (traced by Pb, Cd, As, and Zn) contributing 0.96 $\mu g\,m^{-3}$ (2.8 %).

A sensitivity study was performed in order to better interpret the PMF sources at BCN. In fact, for the period 2007–2014, separate OC and EC measurements were available, and PMF was performed over this period. The comparison between the PMF source contributions obtained using the period 2007–2014 (separate OC and EC measurements) and the whole period (2004–2014; C_{nm} (non-mineral carbon) available) is reported in the Supplement (Fig. S4). As reported

Table 4. Mann–Kendall and multi-exponential trends of source contributions in PM_{10} from PMF at BCN (italic) and MSY. Type: linear (L), single exponential (SE), double exponential (DE); a (μgm^{-3}) and τ (yr) are the constants and the characteristic times, respectively, of the exponential data fittings; NL (%) is the nonlinearity; TR (%) is the total reduction; RC (%) is the residual component; ni denotes not included. Significance of the trends following the Mann–Kendall test: *** (p value < 0.001), ** (p value < 0.01), * (p value < 0.05), + (p value < 0.1).

	PM_{10} (BCN; MSY)		Mann–Kendall fit				Multi-exponential fit				
Source	Contribution 2004 (μgm^{-3})	Contribution 2014 (μgm^{-3})	Fit type	NL (%)	p value	Trend ($\mu gm^{-3}\,yr^{-1}$)	a (μgm^{-3})	τ (yr)	Trend ($\mu gm^{-3}\,yr^{-1}$)	TR (%)	RC (%)
Secondary sulfate	*10.27*	*3.38*	DE	*45*	**		*12.33*	*1.65*	*−0.71*	*67*	*16*
							3.82	*105.80*			
	6.57	3.07	SE	12	**		5.99	13.22	−0.32	53	21
Secondary nitrate	*6.99*	*1.96*	SE	*14*	***		*8.54*	*8.96*	*−0.51*	*67*	*13*
	2.03	0.47	SE	15	**		2.44	8.59	−0.15	69	17
V–Ni-bearing	*4.23*	*1.84*	SE	*11*	**		*5.66*	*10.59*	*−0.32*	*61*	*19*
	0.79	0.44	L	8	**	−0.07				64	25
Industrial/metallurgy (BCN)	*1.64*	*0.71*	SE	*21*	***		*1.76*	*9.56*	*−0.10*	*65*	*16*
Mineral	ni	ni									
	3.46	2.32	L	5	+	−0.10				30	21
Industrial/traffic (MSY)	2.08	1.01	L	7	**	−0.11				56	13

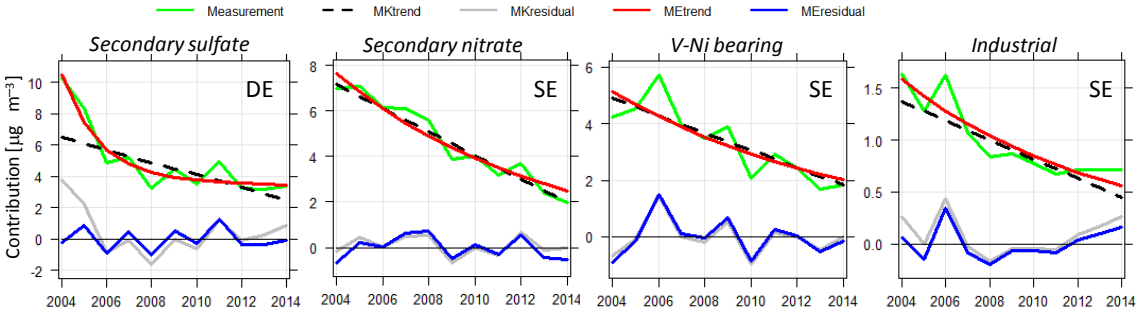

Figure 6. Mann–Kendall and multi-exponential trends for source contributions in PM_{10} at BCN. Measured concentration (green line); multi-exponential trend (red line); multi-exponential residuals (blue line); Mann–Kendall trend (black line); Mann–Kendall residuals (gray line). Trend type: linear (L), single exponential (SE), double exponential (DE). The source contributions at BCN from mineral, traffic, and road/work resuspension were excluded from the trend discussion.

in Fig. SI-4, the relative differences in source contributions ranged from −3 % (Mineral source) to +20 % (industrial source), and R^2 ranged from 0.894 to 0.997, thus confirming the correct interpretation of the 2004–2014 PMF sources where C_{nm} was used. The OC : EC ratio in the traffic source from 2007 to 2014 PMF was 1.70 (cf. Fig. S5), whereas the mean and median OC : EC ratios from chemistry data were 2.5 and 2.3, respectively, thus being in agreement with the contribution of fresh particles from the traffic source at BCN.

4.1 Trends of annual PM_{10} source contributions

Figures 6 and 7 and Table 4 show the results from MK or ME tests applied to the annual averages of PM_{10} source contributions at BCN and MSY. As already noted we cannot study trends for traffic, road/work resuspension, and mineral source contributions at BCN because of the change of the station location in 2009. The contributions that showed statistically significant downward trends at both stations were from secondary sulfate, secondary nitrate, and V–Ni-bearing sources ($p < 0.001$ or $p < 0.01$). Moreover, statistically significant decreasing trends were observed for the industrial/traffic ($p < 0.01$) and mineral ($p < 0.1$) source contributions at MSY and for the industrial/metallurgy source contribution ($p < 0.001$) at BCN. These sources were mostly linked with anthropogenic activities, and the observed decreasing trends confirmed the effectiveness of pollution control measures together with the possible effect of the economic crisis in Spain from 2008. Conversely, the contributions from sources mostly linked with natural processes such as aged marine (at both BCN and MSY) and aged organic (at MSY) did not show statistically significant trends.

The trends of the secondary sulfate source contributions were DE and SE at BCN and MSY, respectively, thus indicating that the decrease over time of this source contribution was not gradual and monotonic. Overall the observed decreasing trends at both stations may be attributed to the legislation that came into force in 2007–2008 in Spain (the EC Directive on Large Combustion Plants), which resulted in the application of flue gas desulfurization (FGD) systems in a number of large facilities. Figure 8 shows the sharp decreases after 2007 observed for the national SO_2 and NO_x emissions

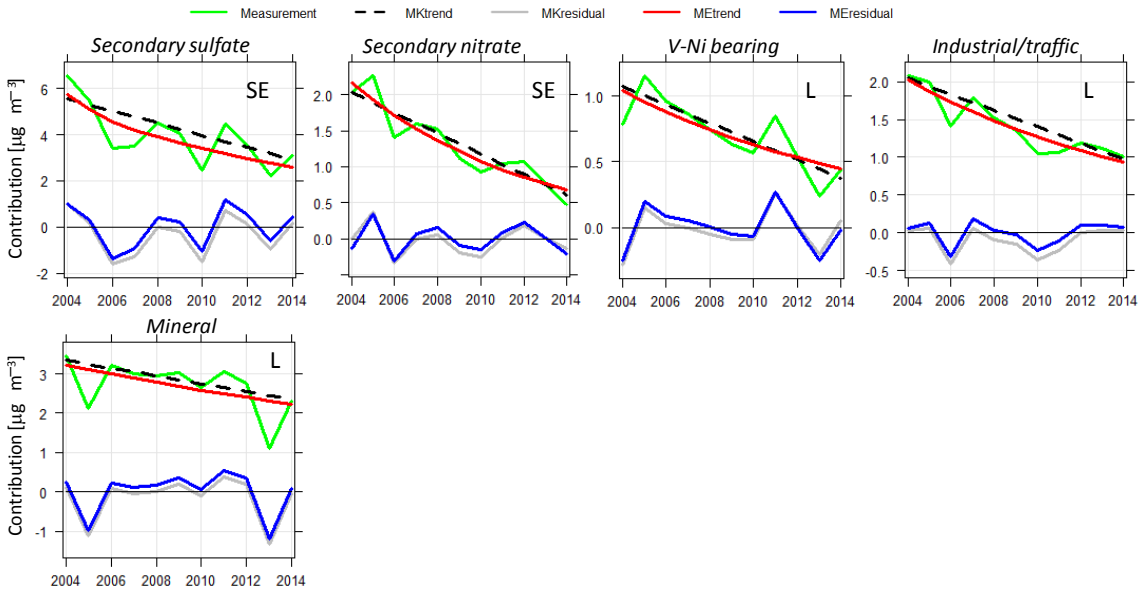

Figure 7. Mann–Kendall and multi-exponential trends for source contributions in PM_{10} at MSY. Measured concentration (green line); multi-exponential trend (red line); multi-exponential residuals (blue line); Mann–Kendall trend (black line); Mann–Kendall residuals (gray line). Trend type: linear (L), single exponential (SE), double exponential (DE).

mostly from power generation (MAGRAMA, 2013; Querol et al., 2014). In BCN the two characteristic times (one low and the other high, cf. Table 4) of the DE fit indicated a strong decrease of the secondary sulfate source contribution at the beginning of the period. This decrease was sharper compared to MSY where the SE fit was used. This difference was mostly due to the ban of heavy oils and petroleum coke for power generation around Barcelona from 2007. The effects of this AQ regional plan were likely more visible in BCN compared to MSY, thus explaining the two different exponential fits used. Overall, for the secondary sulfate source contributions, the TRs were rather high around 53 at MSY and 67 % at BCN, with RC ranging from 16 (BCN) to 21 % (MSY). The fact that the trend of the secondary sulfate source contribution was exponential likely suggested the attainment of a lower limit, and indicated a limited scope for further reduction of SO_2 emissions in our region. In fact, it has been estimated that the maximum in EU will be a further 20 % reduction through measures in industry, residential and commercial heating, and reduced agricultural waste burning (UNECE, 2016). Conversely, in eastern European countries the scope for reduction is much greater and around 60 % (UNECE, 2016).

The trends of the secondary nitrate source contributions were SE at both stations with very similar τ (8.96–8.59 years), TR (67–69 %), and RC (13–17 %). The decrease observed for the contribution from the secondary nitrate source was related to the reduction in ambient NO_x concentrations (Figs. 8 and 9). Figure 9 shows the levels of tropospheric NO_2 column from 2005 to 2014 in southern Europe from NASA NO_2 Ozone Monitoring Instrument (OMI) Level 3 plotted using the Giovanni online data system (Acker and Leptoukh, 2007). In Spain, a general decrease of the concentrations of columnar NO_2 at regional level can be observed. Overall, the implementation of European directives affecting industrial and power generation emissions as well as the increase of the proportion of energy produced from renewable sources (cf. Fig. 10 for Spain), among others, produced a significant reduction of SO_2 and NO_x emissions. Around Barcelona the observed decreases were also attributed to the decrease of NO_x emissions, mainly from the five power generation plants around the city. Moreover, the implementation of the regional AQ Plan for SCRT (continuously regenerating PM traps with selective catalytic reduction for NO_2) and the hybridization and shift to natural gas engines of Barcelona's bus fleet may have had an influence in the observed reductions.

The decreasing trends ($p < 0.01$) of the V–Ni-bearing source contributions were SE and L at BCN and MSY, respectively, reflecting the trends observed at both stations for the concentrations of V and Ni (cf. Table 2). At BCN the characteristic times (τ) were very similar to the characteristic times calculated for PM_{10} V and Ni (cf. Table 2), which were the main tracers of this source. TRs were around 61 % at BCN and 64 % at MSY, and RCs were similar (19–25 %). The observed decrease in the V–Ni-bearing source contribution was mainly attributed to the ban of the use of heavy oils and petroleum coke for power generation in Spain from 2008.

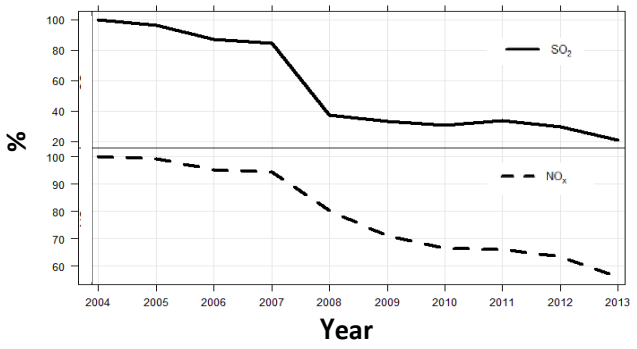

Figure 8. Spanish national emission of SO_2 and NO_x (normalized to year 2004).

The industrial/metallurgy source contribution at BCN decreased exponentially (SE) at the rate of $-0.10\,\mu g\,m^{-3}\,yr^{-1}$ ($p < 0.001$), reflecting the SE decreasing trends observed for the main tracers of this pollutant source (Pb, Cd, and As; cf. Table 2). The decrease of industrial emissions was mainly attributed to the implementation of the IPPC (Integrated Pollution Prevention and Control) Directive. Moreover, the observed decrease may be attributed to a decrease in the emissions from industrial production (smelters; Querol et al., 2007) at a regional scale around Barcelona. Also, the financial crisis, whose impact on industrial production and use of fuels has been evident since October 2008 also contributed to the observed trend. TR and RC for the industrial source contributions at BCN were 65 and 16 %, respectively. As for the contributions from secondary sulfate and nitrate sources, the exponential trend observed for the industrial/metallurgy source contribution suggested the attainment of a lower limit. As evidenced in Fig. 6, the contribution from this source from 2010 was quite low and rather constant.

The contribution of the industrial/traffic source at MSY showed similar magnitude of the trend ($-0.11\,\mu g\,m^{-3}\,yr^{-1}$ with $p < 0.01$) compared to the BCN industrial/metallurgy contribution, both sources being traced mostly by the same industrial tracers. However, this source at MSY was also traced by traffic tracers (i.e., Cu and Sn), which decreased linearly with time (cf. Table 2), thus likely explaining the linear trend observed for the contribution of this source at MSY. TR and RC were 56 and 13 %, respectively, similar to those calculated for the industrial source contribution at BCN.

Finally, the mineral source contribution at MSY showed linear slightly significant decreasing trend ($p < 0.1$) in agreement with that observed at the same station by Cusack et al. (2012). As already noted in Sect. 3.3, this negative trend could be due to both a possible decrease of the emissions of finer anthropogenic mineral species from specific sources, such as cement and concrete production and construction works, and unusual weather conditions, reducing the Saharan dust contribution to PM and resuspension of dust.

In order to further interpret the observed trends, annual data on the annual National Energy Consumption (NECo) from different energy sources (MINETUR, 2013) were also evaluated (Fig. 10). Overall, the primary energy consumption in Spain (NECo statistical data for Spain-MINETUR, 2013) increased from 2004 to 2007 and decreased from 2007, with a marked decrease in 2009. From 2009, the energy consumption indicator remained rather low and constant until 2012, when an additional decrease in 2013 and 2014 was observed. Oil consumption was fairly constant during 2004–2007, showing an important decrease during 2008–2014. This trend was probably governed by the fuel consumption for traffic road. Coal consumption remained constantly high from 2004 to 2007, whereas, as for the emissions of SO_2 (Fig. 8), a sharp decrease occurred from 2007. However, in the period 2011–2014, there was an important increase of coal consumption leading to an average consumption similar to the year 2008. However, the implementation of FGD systems contributed to maintain SO_2 at low concentrations, even in the coal production regions in Spain (cf. Querol et al., 2014). The hydroelectric generation was rather specular to coal consumption. For example, the increase in 2010 of hydroelectric consumption, due to high rainfall rate, mirrored the decrease in the coal consumption observed the same year. Finally, renewable energy consumption increased by 440 % from 2004 to 2014, with a gradual growth in the NECo.

5 Conclusions

PM chemical speciated data collected at two twin stations in the NE of Spain (Barcelona: urban background station and Montseny: regional background station) during 2004–2014 were used to study the trends of the contributions of pollutant sources from PMF model and of their chemical tracers. Despite the fact the trends of different PM fractions ($PM_{2.5}$ and PM_{10}) were linear during the period under study, the trends of specific chemical elements and source contributions were exponential, demonstrating the different effectiveness and/or time of implementation of the different mitigation strategies. Statistically significant exponential trends ($p < 0.01$ or 0.001) were mainly observed for the industrial tracers (Pb, Cd, As) in both PM_{10} and $PM_{2.5}$ and at both sites. The concentrations of V and Ni showed exponential trends in BCN and linear trends at MSY, likely because of the higher distance of the MSY station to the sources of V and Ni (shipping and, before 2008, energy production) compared to BCN. Traffic tracers at MSY (Sn, Cu) showed very similar linear decreasing trends, with higher magnitude of the trends in the fine ($PM_{2.5}$) fractions compared to PM_{10}, likely because of possible sources of coarser Sn and Cu reducing the magnitude of the trends in the PM_{10} mass fraction. The concentrations of Sb at MSY showed a marked exponential decreasing trend compared to other traffic tracers (Cu and Sn), which could be explained by a possible progressive reduction of Sb content

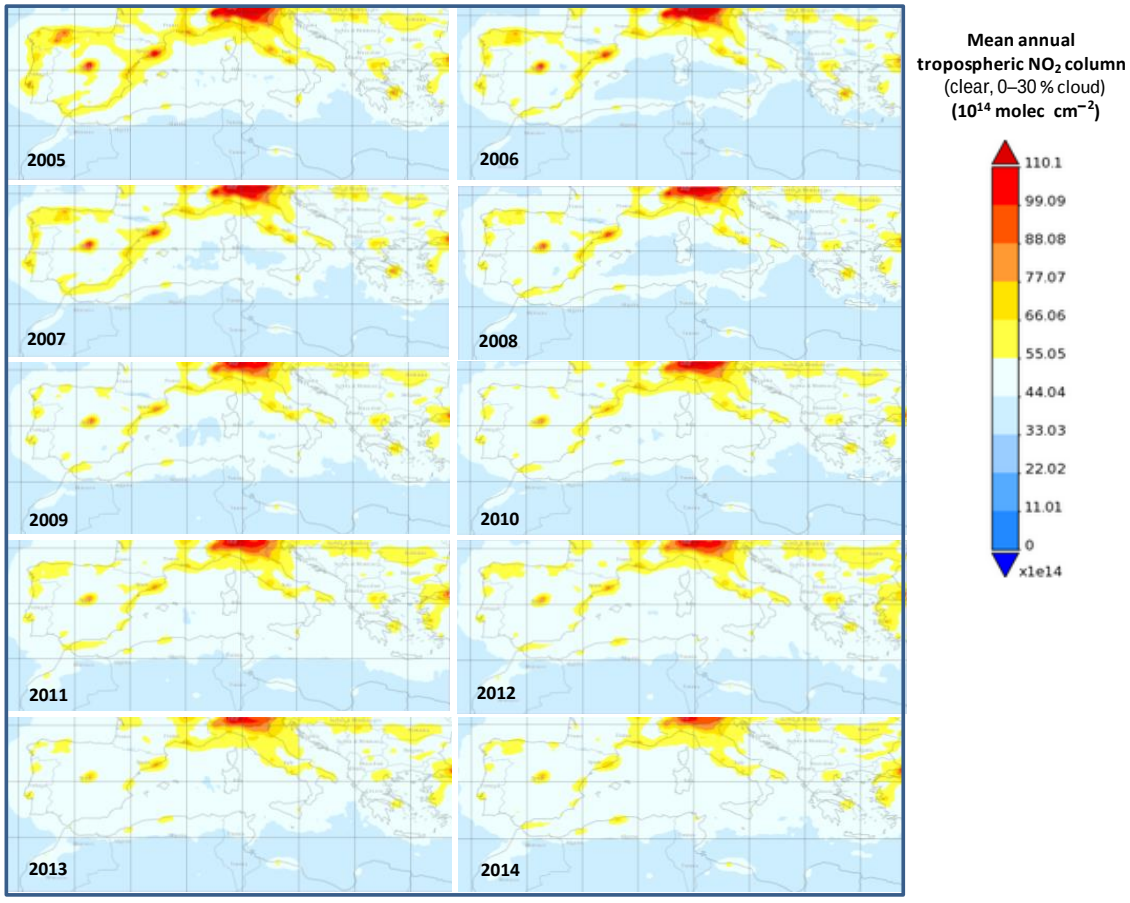

Figure 9. NASA OMI Level 3 tropospheric NO_2 column plotted using the Giovanni online data system, developed and maintained by the NASA GES DISC.

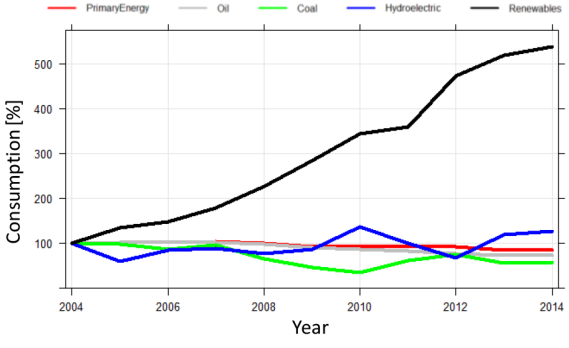

Figure 10. Annual (2004–2014) energy consumption for Spain (normalized to year 2004). Data from the Spanish Ministry of Industry (MINETUR, 2013).

in vehicle brakes. Secondary inorganic aerosols (SO_4^{2-}, NO_3^- and NH_4^+) also showed marked decreasing trends (both linear and exponential) in both fractions and at both sites. However, in general the magnitude of the trends for these species and their statistical significance were higher at BCN compared to MSY.

The PM_{10} source contributions that showed statistically significant downward trends at both Barcelona (BCN; UB) and Montseny (MSY; RB) were from secondary sulfate,secondary nitrate, and V–Ni-bearing sources. For these source contributions, the decreasing trends were exponential, indicating that the trends were not gradual and consistent over time and that the effectiveness of the control measures for these pollutants was stronger at the beginning of the period under study (2004–2009 approximately) compared to the end of the period considered. Statistically significant decreasing trends were observed for the contributions from industrial/traffic and mineral sources at MSY and from the industrial/metallurgy source at BCN. These sources were mostly linked with anthropogenic activities, and the observed decreasing trends confirmed the effectiveness of pollution control measures implemented at European or regional/local levels. The economic crisis which started in 2008 in Spain also contributed to the observed trends. Conversely, the contributions from sources mostly linked with natural processes

such as aged marine (at both BCN and MSY) and aged organic (at MSY) did not show statistically significant trends. The general trends observed for the calculated PMF source contributions reflected the trends observed for the chemical tracers of these pollutant sources well. The decrease in the secondary sulfate source contribution was mainly attributed to the EC Directive on Large Combustion Plants implemented in Spain from 2008, resulting in the application of flue gas desulfurization (FGD) systems in a number of large facilities. Moreover, according to the 2008 regional AQ plan, the use of heavy oils and petroleum coke for power generation was forbidden around Barcelona from 2008 in favor of natural gas. As a consequence, a decrease of the contributions from the V–Ni-bearing source at both sites was also observed. The decrease observed for the contribution of the secondary nitrate source was mainly due to the reduction in ambient NO_x concentrations. In Spain a general decrease of the concentrations of NO_2 at regional level was observed, and it was mainly related with the lower energy consumption related with the financial crisis. The decrease of nitrates concentrations and secondary nitrate source contributions around Barcelona was also attributed to the decrease of NO_x emissions from the five power generation plants around the city. Moreover, a regional AQ plan implementing the SCRT (continuously regenerating PM traps with selective catalytic reduction for NO_2) and the hybridization and shift to natural gas engines of Barcelona's bus fleet may have also had an influence on NO_x ambient concentrations. The industrial/metallurgy source contribution at BCN decreased exponentially, reflecting the exponential trends observed for the main tracers of this pollutant source (Pb, Cd and As). The implementation of the IPPC (Integrated Pollution Prevention and Control) Directive, together with a decrease in the emissions from industrial production (smelters) at a regional scale around Barcelona, explained the observed trends. Overall, the magnitudes of the decreasing trends of the contributions of the pollutant sources were higher at BCN compared to MSY, likely because of the proximity of the BCN measurement site to anthropogenic pollutant sources compared to the MSY site. The results presented in this work clearly confirm the beneficial effect of the AQ measures taken in recent years in Europe. However, the WHO limit values of specific pollutants, such as PM_{10} and $PM_{2.5}$, are still exceeded, especially at urban level and industrial hotspots. To meet the WHO guide levels, important action is still required for the next decade and the interpretation of past air quality trends may yield relevant outcomes for planning further cost-effective actions. We would like to highlight that a non-linear approach to trend studies is very attractive, given that some air pollutants reported in this work showed reductions that are not gradual with time. Conversely, for specific pollutant source-contribution/concentration in our region, the decreasing trends were less steep at the end of the period compared to the beginning, thus likely indicating the attainment of a lower limit. This was the case, for example, for the secondary sulfate source contribution decreasing exponentially from 2004 to 2014, thus likely indicating a limited scope for further reduction of SO_2 emissions in our region.

6 Data availability

The Montseny data sets used for this publication are accessible online on the following web page: www.http://ebas.nilu.no/. The Barcelona data sets were collected within different national/regional projects and/or agreements and are available upon request.

The Supplement related to this article is available online at doi:10.5194/acp-16-11787-2016-supplement.

Acknowledgements. This work was supported by the MINECO (Spanish Ministry of Economy and Competitiveness), the MAGRAMA (Spanish Ministry of Agriculture, Food and Environment), the Generalitat de Catalunya (AGAUR 2014 SGR33 and the DGQA), and FEDER funds under the PRISMA project (CGL2012-39623-C02/00). The research leading to these results has received funding from the European Union's Horizon 2020 research and innovation programme under grant agreement no. 654109 and previously from the European Union Seventh Framework Programme (FP7/2007-2013) under grant agreement no. 262254. Marco Pandolfi is funded by a Ramón y Cajal Fellowship (RYC-2013-14036) awarded by the Spanish Ministry of Economy and Competitiveness. NO_2 map analyses and visualizations used in this paper were produced with the Giovanni online data system, developed and maintained by the NASA GES DISC. The authors would like to express their gratitude to D. C. Carslaw and K. Ropkins for providing the Openair software used in this paper (Carslaw and Ropkins, 2012; Carslaw, 2012).

Edited by: V.-M. Kerminen
Reviewed by: three anonymous referees

References

Acker, J. G. and Leptoukh, G.: Online Analysis Enhances Use of NASA Earth Science Data, Eos, Trans. AGU, 88, 14–17, 2007.

Alastuey, A., Minguillón, M. C., Pérez, N., Querol, X., Viana, M., and de Leeuw, F.: PM10 Measurement Methods and Correction Factors: 2009 Status Report, ETC/ACM Technical Paper 2011/21, 2011.

Amato, F., Pandolfi, M., Escrig, A., Querol, X., Alastuey, A., Pey, J., Perez, N., and Hopke, P. K.: Quantifying road dust resuspension in urban environment by Multilinear Engine: A comparison with PMF2, Atmos. Environ., 43–17, 2770–2780, 2009.

Barmpadimos, I., Keller, J., Oderbolz, D., Hueglin, C., and Prévôt, A. S. H.: One decade of parallel fine ($PM_{2.5}$) and coarse (PM_{10}-$PM_{2.5}$) particulate matter measurements in Europe: trends and variability, Atmos. Chem. Phys., 12, 3189–3203, doi:10.5194/acp-12-3189-2012, 2012.

Carslaw, D. C.: The OpenAir manual – open-source tools for analysing air pollution data, Manual for version 0.5–16, King's College, London, 2012.

Carslaw, D. C. and Ropkins, K.: OpenAir – an R package for air quality data analysis, Environ. Model Softw., 27–28, 52–61, 2012.

Cavalli, F., Viana, M., Yttri, K. E., Genberg, J., and Putaud, J.-P.: Toward a standardised thermal-optical protocol for measuring atmospheric organic and elemental carbon: the EUSAAR protocol, Atmos. Meas. Tech., 3, 79–89, doi:10.5194/amt-3-79-2010, 2010.

Cusack, M., Alastuey, A., Pérez, N., Pey, J., and Querol, X.: Trends of particulate matter ($PM_{2.5}$) and chemical composition at a regional background site in the Western Mediterranean over the last nine years (2002–2010), Atmos. Chem. Phys., 12, 8341–8357, doi:10.5194/acp-12-8341-2012, 2012.

EEA: European Environmental Agency Air quality in Europe – 2013 report, EEA report 9/2013, Copenhagen, 1725–9177, available at: http://www.eea.europa.eu/publications/air-quality-in-europe-2013 (last access: 10 March 2016), 2013.

EEA: European Environmental Agency Air quality in Europe – 2015 report, Many Europeans still exposed to harmful air pollution, Air pollution is the single largest environmental health risk in Europe, EEA report 11/2015, Copenhagen, 1–7, available at: http://www.eea.europa.eu/media/newsreleases/many-europeans-still-exposed-to-air-pollution-2015 (last access: 16 May 2016), 2015.

Escrig, A., Monfort, E., Celades, I., Querol, X., Amato, F., Min guillon, M. C., and Hopke, P. K.: Application of optimally scaled target factor analysis for assessing source contribution of ambi ent PM10, J. Air Waste Manage., 59, 1296–1307, 2009.

Gilbert, R. O.: Statistical Methods for Environmental Pollution Monitoring, Wiley, NY, 1987.

Guerreiro, C., Leeuw, F. de, Foltescu, V., Horálek, J., and European Environment Agency: Air quality in Europe 2014 report, Luxembourg: Publications Office, available at: http://bookshop.europa.eu/uri?target=EUB:NOTICE:THAL14005:EN:HTML (last access: 2 June 2016), 2014.

Harrison, R. M., Stedman, J., and Derwent, D.: New directions: why are PM10 concentrations in Europe not falling?, Atmos. Environ., 42, 603–606, 2008.

Henschel, S., Querol, X., Atkinson, R., Pandolfi, M., Zeca, A., Le Tertre, A., Analitis, A., Katsouyanni, K., Chanel, O., Pascal, M., Bouland, C., Haluza, D., Medina, S., and Goodman, P. G.: Ambient air SO_2 patterns in 6 European cities, Atmos. Environ., 79, 236–247, 2013.

Henschel, S., Le Tertre, A., Atkinson, R.W., Querol, X., Pandolfi, M., Zeka, A., Haluza, D., Antonis, A., Katsouyanni, K., Bouland, C., Pascal, M., Medina, S., and Goodman, P. G.: Trends of nitrogen oxides in ambient air in nine European cities between 1999 and 2010, Atmos. Environ., 117, 234–241, 2015.

Kendall, M. G.: Rank Correlation Methods, 4th Edn., Charles Griffin, London, 1975.

MAGRAMA: Inventario Nacional de Emisiones de Contaminantes a la Atmósfera, Ministerio de Agricultura, Alimentación y Medio Ambiente del Gobierno de España, available at: http://www.magrama.gob.es/ca/calidad-y-evaluacion-ambiental/temas/sistemaespanol-de-inventario-sei-/ (last access: 12 February 2016), 2013.

Mann, H. B.: Non-parametric tests against trend, Econometrica, 13, 163–171, 1945.

MINETUR: Ministerio de Industria, Energía y Turismo, Gobierno de España: energy statistics and balances, available at: http://www.minetur.gob.es/energia/balances/Balances/Paginas/CoyunturaTrimestral.aspx (last access: 12 February 2016), 2013.

Paatero, P.: Least squares formulation of robust non-negative factor analysis, Chemometr. Intell. Lab., 37, 23–35, 1997.

Paatero, P.: User's guide for positive matrix factorization programs PMF2 and PMF3, Part 1: tutorial, University of Helsinki, Helsinki, Finland, 2004.

Paatero, P. and Tapper, U.: Positive Matrix Factorization: a non negative factor model with optimal utilization of error estimates of data values, Environmetrics, 5, 111–126, 1994.

Paatero, P. and Hopke, P. K.: Discarding or downweighting high noise variables in factor analytic models, Anal. Chim. Ac., 490, 277–289, doi:10.1016/s0003-2670(02)01643-4, 2003.

Paatero, P., Hopke, P. K., Song, X., and Ramadan, Z.: Understanding and controlling rotations in factor analytic models, Chemometr. Intell. Lab., 60, 253–264, 2002.

Paatero, P., Hopke, P. K., Begum, B. A., and Biswas, S. K.: A graphical diagnostic method for assessing the rotation in factor analytical models of atmospheric pollution, Atmos. Environ., 39, 193–201, doi:10.1016/j.atmosenv.2004.08.018, 2005.

Pandolfi, M., Cusack, M., Alastuey, A., and Querol, X.: Variability of aerosol optical properties in the Western Mediterranean Basin, Atmos. Chem. Phys., 11, 8189–8203, doi:10.5194/acp-11-8189-2011, 2011.

Pandolfi, M., Amato, F., Reche, C., Alastuey, A., Otjes, R. P., Blom, M. J., and Querol, X.: Summer ammonia measurements in a densely populated Mediterranean city, Atmos. Chem. Phys., 12, 7557–7575, doi:10.5194/acp-12-7557-2012, 2012.

Pandolfi, M., Martucci, G., Querol, X., Alastuey, A., Wilsenack, F., Frey, S., O'Dowd, C. D., and Dall'Osto, M.: Continuous atmospheric boundary layer observations in the coastal urban area of Barcelona during SAPUSS, Atmos. Chem. Phys., 13, 4983–4996, doi:10.5194/acp-13-4983-2013, 2013.

Pandolfi, M., Querol, X., Alastuey, A., Jimenez, J. L., Jorba, O., Day, D., Ortega, A., Cubison, M. J., Comerón, A., Sicard, M., Mohr, C., Prévôt, A. S. H., Minguillón, M. C., Pey, J., Baldasano, J. M., Burkhart, J. F., Seco, R., Peñuelas, J., van Drooge, B. L., Artiñano, B., Di Marco, C., Nemitz, E., Schallhart, S., Metzger, A., Hansel, A., Lorente, J., Ng, S., Jayne, J., and Szidat, S.: Effects of sources and meteorology on particulate matter in the Western Mediterranean Basin: An overview of the DAURE campaign, J. Geophys. Res.-Atmos., 119, 4978–5010, doi:10.1002/2013JD021079, 2014.

Pérez, N., Pey, J., Castillo, S., Viana, M., Alastuey, A., and Querol, X.: Interpretation of the variability of levels of regional background aerosols in the Western Mediterranean, Sci. Total Environ., 407, 527–540, doi:10.1016/j.scitotenv.2008.09.006, 2008.

Pey, J., Pérez, N., Querol, X., Alastuey, A., Cusack, M., and Reche, C.: Intense winter atmospheric pollution episodes affecting the Western Mediterranean, Sci. Total Environ., 408, 1951–9, doi:10.1016/j.scitotenv.2010.01.052, 2010.

Pey, J., Querol, X., Alastuey, A., Forastiere, F., and Stafoggia, M.: African dust outbreaks over the Mediterranean Basin during 2001–2011: PM10 concentrations, phenomenology and trends,

and its relation with synoptic and mesoscale meteorology, Atmos. Chem. Phys., 13, 1395–1410, doi:10.5194/acp-13-1395-2013, 2013.

Querol, X., Viana, M., Alastuey, A., Amato, F., Moreno, T., Castillo, S., Pey, J., de la Rosa, J., Artíñano, B., Salvador, P., García Dos Santos, S., Fernández-Patier, R., Moreno-Grau, S., Negral, L., Minguillón, M. C., Monfort, E., Gil, J. I., Inza, A., Ortega, L. A., Santamaría, J. M., and Zabalza, J.: Source origin of trace elements in PM from regional background, urban and industrial sites of Spain, Atmos. Environ., 41, 7219–7231, 2007.

Querol, X., Alastuey, A., Moreno, T., Viana, M.M., Castillo, S., Pey, J., Rodríguez, S., Artiñano, B., Salvador, P., Sánchez, M., Garcia Dos Santos, S., Herce Garraleta, M. D., Fernandez-Patier, R., Moreno-Grau, S., Negral, L., Minguillón, M. C., Monfort, E., Sanz, M. J., Palomo-Marín, R., Pinilla-Gil, E., Cuevas, E., de la Rosa, J., and Sánchez de la Campa, A.: Spatial and temporal variations inairborne particulate matter (PM10 and PM2.5) across Spain 1999–2005, Atmos. Environ., 42, 3694–3979, 2008.

Querol, X., Viana, M., Moreno, T., Alastuey, A., Pey, J., Amato, F., Pandolfi, M., Minguillón, M. C., Reche, C., Pérez, N., González, A., Pallarés, M., Moral, A., Monfort, E., Escrig, A., Cristóbal, A., Hernández, I., Miró, J. V., Jiménez, S., Reina, F., Jabato, R., Ballester, F., Boldo, E., and Bellido, J.: Scientific bases for a National Air Quality Plan (in Spanish), Colección Informes CSIC, 978-84-00-09475-1, 2012.

Querol, X., , Alastuey, A., Pandolfi, M., Reche, C., Pérez, N., Minguillón, M. C., Moreno, T., Viana, M., Escudero, M., Orio, A., Pallarés, M., and Reina, F.: 2001–2012 trends on air quality in Spain, Sci. Total Environ., 490, 957–969, doi:10.1016/j.scitotenv.2014.05.074, 2014.

Salmi, T., Maata, A., Antilla, P., Ruoho-Airola, T., and Amnell, T.: Detecting trends of annual values of atmospheric pollutants by the Mann Kendall test and Sen's slope estimates – the Excel template application Makesens, Finnish Meteorological Institute, Helsinki, Finland, 35 pp., 2002.

Salvador P., Artíñano B., Viana M., Alastuey A., and Querol X.: Evaluation of the changes in the Madrid metropolitan area influencing air quality: analysis of 1999–2008 temporal trend of Particulate Matter, Atmos. Environ., 57, 175–185, 2012.

Sen, P. K.: Estimates of regression coefficient based on Kendall's tau, J. Am. Stat. Assoc., 63, 1379–1389, 1968.

Shatalov, V., Ilyin I., Gusev A., Rozovskaya O., and Travnikov O.: Heavy Metals and Persistent Organic Pollutants: development of multi-scale modeling and trend analysis methodology, EMEP/MSC-E Technical report 1/2015, 2015.

Smith, D. M.: Computing single parameter transformations, Communications in Statistics – Simulation and Computation, 32, 605–618, 2002.

Theil, H.: A rank invariant method of linear and polynomial regression analysis, I, II, III, Proceedings of the Koninklijke Nederlandse Akademie Wetenschappen, Series A, Mathematical Sciences, 386–392, 521–525, 1397–1412, 1950.

UNECE: Towards Cleaner Air. Scientific Assessment Report. EMEP Steering Body and Working Group on Effects of the Convention on Long-Range Transboundary Air Pollution, Oslo, 50 pp., edited by: Maas, R. and Grennfelt, P., www.unece.org/environmental-policy/conventions/envlrtapwelcome/publications.html (last access: 3 July 2016), 2016.

Williams, M. L. and Carslaw, D.: New directions: science and policy – out of step on NO_x and NO_2?, Atmos. Environ., 45, 3911–3912, 2011.